Available online at BCREC website: https://bcrec.id

Bulletin of Chemical Reaction Engineering & Catalysis, 15 (1) 2019, 35-42

Research Article

One-pot Synthesis of Carbon-doped TiO_2 with Bimetallic Ni-Ag Co-catalysts in Photodegradation of Methylene Blue under UV and Visible Irradiation

Kurnia Putri[1], A. Annisa[1], Sadang Husain[2], R. Rodiansono[1]*

[1]Department of Chemistry, Lambung Mangkurat University, Jl. A. Yani Km 36 Banjarbaru 70714, Tel./fax: +62-511-477 3112, Indonesia
[2]Department of Physics, Lambung Mangkurat University, Jl. A. Yani Km 36 Banjarbaru 70714, Tel./fax: +62-511-477 3112, Indonesia

Received: 1st May 2019; Revised: 20th August 2019; Accepted: 23rd August 2019; Available online: 28th February 2020; Published regularly: April 2020

Abstract

Carbon modified-titanium dioxide (@C-TiO_2) was prepared by one-pot procedure from $TiCl_4$ and glucose under hydrothermal conditions at 150 °C for 24 hours. The obtained @C-TiO_2 was employed as support for Ni-Ag(3.0)@C-TiO_2 nanocomposite (3.0 is the Ni/Ag molar ratio). The synthesized catalysts were characterized by means of XRD and UV-Vis DRS Spectroscopy. The XRD patterns of @TiO_2 show the brookite as the main phase, meanwhile the main phase in the @C-TiO_2, Ni-Ag(3.0)@TiO_2 and Ni-Ag(3.0)@C-TiO_2 nanocomposites were anatase. The band gap of the TiO_2 sample slightly shifted to the visible range after the addition of C dopant or Ni-Ag(3.0) co-catalyst as indicated by UV-Vis DRS spectra. Ni-Ag(3.0)@C-TiO_2 catalyst showed high photocatalytic activity for photodegradation of MB under both UV and visible irradiations at 60 °C within 2 hours with maximum MB conversion of 67.5% and 54.1%, respectively. The synergistic action of C dopant or Ni-Ag(3.0) co-catalyst is believed to be important in the improvement of photocatalytic activity of @TiO_2.

Keywords: C-doped TiO_2; bimetallic Ni-Ag co-catalyst; methylene blue; photodegradation

How to Cite: Putri, K., Annisa, A., Husain, S., Rodiansono, R. (2020). One-pot Synthesis of Carbon-doped TiO_2 with Bimetallic Ni-Ag co-catalysts in Photodegradation of Methylene Blue under UV and Visible Irradiation. *Bulletin of Chemical Reaction Engineering & Catalysis*, 15(1): 35-42 (doi:10.9767/bcrec.15.1.4811.35-42)

Permalink/DOI: https://doi.org/10.9767/bcrec.15.1.4811.35-42

1. Introduction

Titanium dioxide (TiO_2)-based photocatalysis as a green chemistry technology has drawn considerable attention due to its extensively potential applications in the fields of organic pollutant degradation, environmental remediation, and solar energy conversion [1-5]. However, the application of pure TiO_2 is limited, because of it requires ultraviolet (UV) light, which makes up only a small fraction (<4%) of the total solar spectrum reaching the surface of the earth. Therefore, over the past few years, considerable efforts have been directed towards the improvement of the photocatalytic efficiency of TiO_2 in the visible-light region [6-8].

There are several notable efforts in the improvement of photocatalytic efficiency of TiO_2 in the visible-light region including the addition of second atoms as dopant both metal and non-metal dopants [8,9]. Various transition metals

* Corresponding Author.
E-mail: rodiansono@ulm.ac.id (R. Rodiansono);
Tel./fax: +62 511 477 3112

dopant have been evaluated, such as: vanadium (V), molybdenum (Mo), rhodium (Rh), and iron (Fe) and among them, iron was widely applied due to Fe^{3+} has ionic radius of 0.79 Å which is very close to ionic radius of Ti^{4+} resulting in easier for doping processes of ion Fe^{3+} into TiO_2 [8-10] and demonstrated relatively high activity on the methylene blue photodecomposition within a 65 min of reaction time [11]. On the other hand, non metal dopants, such as: nitrogen (N), sulphur (S), and carbon (C) are also frequently employed to improve the sensitivity of TiO_2 towards visible-light resources [12-13]. For example, carbon doped-TiO_2 (C-TiO_2) with amount of carbon-doped around 5.2 %mol has lowest band-gap energy of 2.3-2.8 eV [12]. Several previous reports have also showed that C-TiO_2 catalysts were effective for the photodecomposition of acid orange 7 (AO7) with 99% conversion [14]. Teng *et al.* also reported the conversion of Rhodamine B using C-TiO_2 catalyst (with band-gap energy of 2.91 eV) and 95% conversion Rhodamine B was achieved under visible-light irradiation [15].

Beside the addition of dopant, the presence of co-catalysts could also enhance the photocatalytic efficiency of TiO_2 under visible light region. Various transition metals have been investigated and a significant improvement was also achieved [17-18]. Zhang *et al*. reported the use of vanadium (V), platinum (Pt), nickel (Ni), and chromium (Cr) as co-catalyst for photodegradation of methyl orange with 60% conversion which is higher than that of pure TiO_2 (30% conversion) [19]. Sung-suh *et al*. reported that the efficiency of Ag-TiO_2 increased almost three times during the photodegradation of Rhodamine under visible-light irradiation [20].

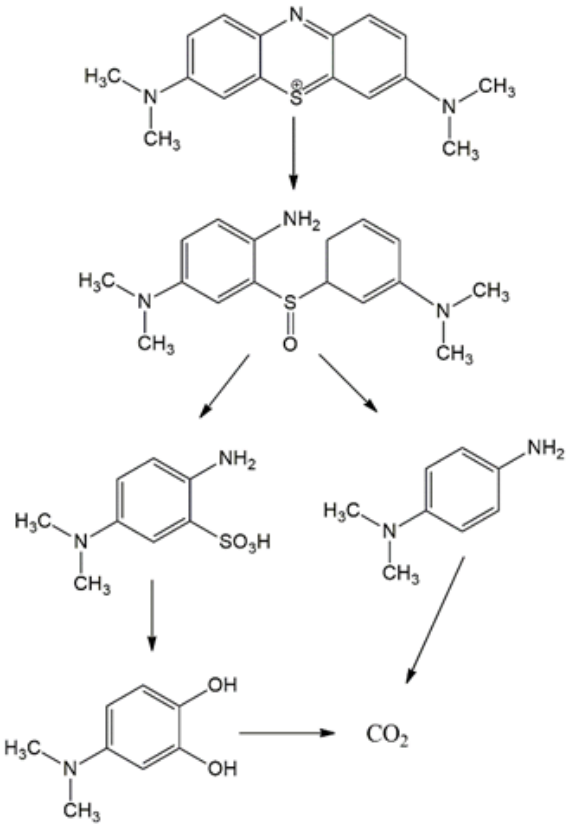

Figure 1. Possible reaction mechanism for MB photodegradation over Ni-Ag(3.0)@C-TiO_2 [16]

In the present work, we report the simple procedure for the synthesis of carbon-doped titanium oxide (@C(5.2%)-TiO_2; 5.2% is amount of C to TiO_2 in %wt) in one pot synthetic protocol from glucose and titanium tetrachloride ($TiCl_4$) as precursors of carbon and TiO_2, respectively, via hydrothermal treatment at 150 ^oC for 24 h. Bimetallic nickel-silver (Ni-Ag(3.0); 3.0 is Ni/Ag molar ratio) catalysts, @both bulk and supported on @TiO_2 and @C-TiO_2, were also synthesized using a similar procedure to the previous reports [21-22]. The synthesized catalysts then were evaluated for the photodegradation of methylene blue in batch reactor system under both ultraviolet (UV) and visible (Vis) light irradiation at 60 ^oC. The effect of reaction conditions and catalyst characterizations are discussed throughout the manuscript text.

2. Materials and Methods

2.1 Materials

Nickel chloride hexahydrate ($NiCl_2.6H_2O$ 99.9%), silver nitrate ($AgNO_3$ 99.8%), NaOH pellet 99.0%, D(+)-Glucose anhydrate, $TiCl_4$ 99.0%, HCl 37%, ethanol 96%, and ethylene glycol (EG) 99.5% were purchased from Merck Millipore and used as received. Sodium borohydrate ($NaBH_4$ 95.0%) and methylene blue 70.0% were purchased from Tokyo Chemical Industry Ltd Co. (TCI).

2.2 Catalyst Preparation

2.2.1 Synthesis of @C-TiO_2

A typical procedure for the synthesis of carbon-doped titanium oxide (@C-TiO_2) is described as follows. A 2.0 M of $TiCl_4$ solution was prepared by diluting 100 mL $TiCl_4$ (99%, Merck) with 1.0 mL HCl 37% in 350 mL of deionized water [23]. Carbon-doped TiO_2 (@C(5.2%-TiO_2; 5.2% %wt of C to TiO_2) was synthesized by mixing a glucose solution (~15 g/L) with 20 mL $TiCl_4$ (0.04 mol) solution at room temperature. The pH of mixture was adjusted by addition of NaOH 10 M dropwise un-

til pH = 10. The mixture was homogenized at 50 °C for 18 h then transferred into an autoclave-Teflon reactor for hydrothermal processes at 150 °C for 24 h. After finished, the reactor was cooled to room temperature and the precipitate was filtered, washed with absolute ethanol and followed by deionized water until pH become neutral and then dried at 80 °C for 3 h to obtain @C-TiO_2 powder.

2.2.2 Synthesis of Ni-Ag(3.0)@C-TiO_2

Synthesis of bimetallic nickel-silver supported on @C-TiO_2 (denoted as Ni-Ag(3.0)@C-TiO_2; 3.0 is Ni/Ag molar ratio) is described as follows [21-22]. A 0.8568 gram $NiCl_2 \cdot 6H_2O$ (3.6 mmol) was dissolved in deionized water (5 mL) (denoted as solution A) and 0.2038 gram $AgNO_3$ (1.2 mmol) was dissolved in deionized water (5 mL) (denoted as solution B). Solution A and B, ethylene glycol (20 mL), NaOH (6 M, 3 mL) were mixed at room temperature while gently stirring while an one gram $NaBH_4$ was also added slowly. The mixture was transferred into an autoclave-Teflon reactor for hydrothermal processes at 150 °C for 24 h. After finished, the reactor was cooled to room temperature and the precipitate was filtered, washed with absolute ethanol and followed by deionized water until pH become neutral and then dried at 110 °C for 3 h to obtain Ni-Ag(3.0)@C-TiO_2 powder.

2.3 Catalyst Characterization

Powder X-ray diffraction (XRD) measurements were recorded on a Mac Science M18XHF instrument using monochromatic Cu-Kα radiation (λ = 0.15418 nm). The XRD equipment operated at 40 kV and 200 mA with a step width of 0.02° and a scan speed of 4° min^{-1} (α1 = 0.1540 nm, α2 = 0.1544 nm).

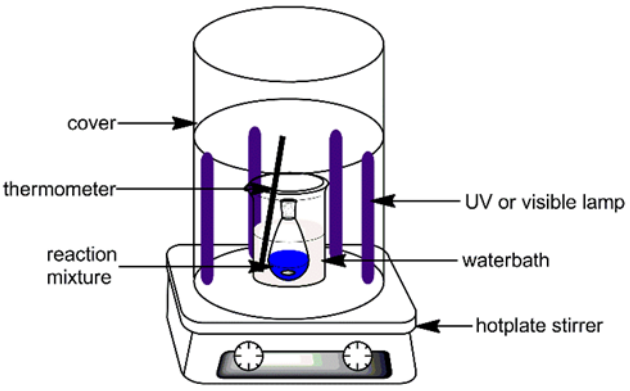

Figure 2. Schematic diagram of the reactor for the photodegradation of methylene blue over carbon-doped TiO_2 with bimetallic Ni-Ag co-catalysts.

Analysis ultraviolet-visible diffuse reflectance spectroscopy (UV-Vis DRS) was performed on an UV-Vis Shimadzu 2450 with double beam system at Affiliation Laboratory of Chemistry, Faculty of Mathematics and Natural Sciences (FMIPA), University of Indonesia Jakarta $BaSO_4$ powder was used as standard material. The calculation of band-gap energy (E_g) was derived from the obtained spectra using a formula of $E_g = h.C/\lambda_C$, whereas h is Planck constant (4.136×10^{-15} eV.s), C is light velocity (2.997×10^{8} $m.s^{-1}$), λ_C is *cut-off* wave length (nm). λ_C was derived from plotted data of absorbance versus wavelength with linear cross-section on the spectra (Tauc plot) [26-27].

The NH_3-TPD was carried out on a Belsorp Max (BEL Japan). The samples were degassed at elevated temperature of 100-200 °C for 2 h to remove physisorbed gases prior to the measurement. The temperature was then kept at 200 °C for 2 h while flushed with He gas. NH_3 gas (balanced NH_3, 80% and He, 20%) was introduced at 100 °C for 30 min, then evacuated by helium gas to remove the physisorbed also for 30 min. Finally, temperature programmed desorption was carried out at temperature of 100-900 °C and the desorbed NH_3 was monitored by TCD.

2.4 Photodegradation of Methylene Blue

A typical procedure for the photodegradation of methylene blue (MB) over Ni-Ag(3.0)@C-TiO_2 catalyst is described as follows. A solution of MB (100 ppm, 30 mL) and 0.15 g Ni-Ag(3.0)@C-TiO_2 were mixed in glass-tube reactor (50 mL) then immersed in water batch at 60 °C under UV or visible irradiations (UV or visible lamp sources are 4 x 8 W). The reaction mixture was stirred at 310 rpm for 30 min to reach the equilibrium point of adsorption-desorption. The reaction mixture was irradiated for 120 min at a reaction temperature of 60 °C and sampled every 30 min and analyzed by using Perkin Elmer UV-Vis double beam spectroscopy.

3. Results and Discussion

3.1 Catalyst Characterizations

Figure 3 shows the XRD patterns of the synthesized titanium oxide (@TiO_2), carbon (@C) and @C-TiO_2 nanocomposite. It can be observed that the brookite phase was predominantly formed in TiO_2 sample. A serial diffraction peak at 2θ = 25.78°, 26.86°, 31.24°, 40.32°,

44.94°, 53.4°, and 55.98° which can be recognized as TiO_2 brookite (120), (111), (121), (022), (032), (320), dan (241), respectively. Anatase phase was also observed at 2θ = 25.04°, 36.94° dan 53.4° which also can be assigned as TiO_2 anatase (101), (103), and (105), respectively. A single diffraction peak at 2θ = 28.10° that characteristic peaks of TiO_2 rutile (110) (Figure 3b). In the case of C-TiO_2 nanocomposite, the main phase of formed-TiO_2 in @C-TiO_2 was anatase which can be easily recognized at 2θ = 24.48°, 36.94°, and 53.48° as TiO_2 anatase (101), (103), and (105), respectively. Ren *et al.* also reported that the use of glucose as precursor of carbon promoted the formation of TiO_2 anatase and inhibited TiO-$_2$ brookite formation [24].

Figure 4 shows the XRD pattern of bulk Ni-Ag(3.0), Ni-Ag(3.0)@TiO_2, and Ni-Ag(3.0)@C-TiO_2. The formation of TiO_2 anatase (101) was observed at 2θ = 25.29° (Figure 4a) which is hardly to calculated the crystallite sizes due to the small peak. A sharp diffraction peak was observed at 2θ = 37.82° which can be recognized as Ag(111) in all samples (Figure 4). A series diffraction peaks at 2θ = 37.82°, 64.20°, and 77.16° which can be assigned as Ag(111), Ag(220), and Ag(311), respectively. Two overlapped peak of bimetallic alloy NiAg(110) and Ni(111)/Ag(200) at diffraction peaks at 2θ = 32.82° and 43.99°, respectively were also clearly observed [25]. The crystallite sizes of Ni-Ag(110), Ag(111), and Ni(111)/Ag(200) in bulk Ni-Ag(3.0) sample were 23.40 nm, 22.73 nm, and 21.50 nm, respectively. In Ni-Ag(3.0)@TiO_2 sample, the crystallite sizes of bimetallic Ni-Ag alloy are unable to calculate using Scherrer equation.

Figure 5 shows the NH_3-TPD spectra of the synthesized @C-TiO_2, (b) Ni-Ag(3.0)@TiO_2, and (c) Ni-Ag(3.0)@C-TiO_2 and the total acidity also summarized in Table 1. The synthesized @TiO_2 has highest amount of acid sites (968 μmolg^{-1}) among the catalysts (entry 1) while the amount of acid sites of @C-TiO_2 nanocomposite slightly decreased to 822 μmolg^{-1} (entry 2). Bulk Ni-Ag@TiO_2 consists of desorption peak at 183°C which can be attributed as a weak acidity. On the other hand, Ni-Ag(3.0)@C-TiO_2 comprises two desorption peaks at 210 °C and 498 °C which can be recognized as weak and medium acidities and the total amount of acid sites was 240 μmolg^{-1} (entry 5).

Figure 6 displays the UV-Vis DRS spectra of each synthesized catalysts. The band-gap energy (E_g) was estimated from the plotting of absorbance (A) versus wavelength (nm) using Tauc plot and a formula of $E_g = h.C/\lambda_C$, whereas h is Planck constant, C is light velocity, λ_C is *cut-off* wave length (nm) that derived from plotted data of absorbance versus wavelength [26-27]. It was found that the estimated band gap energies (E_g) of each synthesized catalysts

Table 1. Physico-chemical properties of @C-TiO_2 and Ni-Ag@C-TiO_2 nanocomposites.

Entry	Catalysts[a]	Total acidiy[b] (mmol.g^{-1})	λ (nm)	*Eg*[c] (eV)
1	@TiO_2	968	419	2.96
2	@C-TiO_2	822	483	2.57
3	Bulk Ni-Ag(3.0)	65	n.d.	n.d.
4	Ni-Ag(3.0)@TiO_2	46	436	2.84
5	Ni-Ag(3.0)@C-TiO_2	240	461	2.69

[a]The value in the parenthesis is Ni/Ag molar ratio.
[b]Total acidity of catalyst derived from NH_3-TPD.
[c]Band gap energy derived from UV-Vis DRS spectra data.

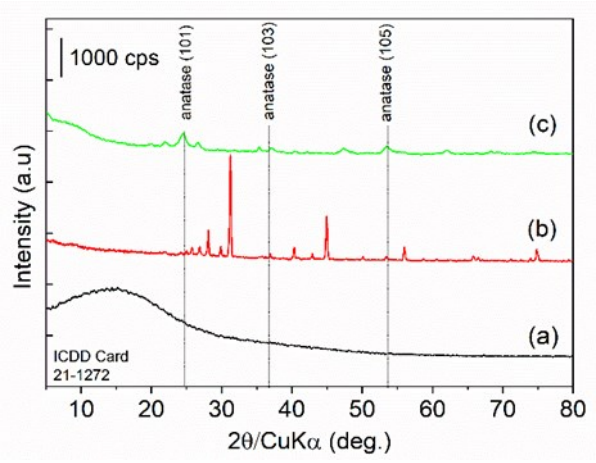

Figure 3. XRD patterns of the synthesized (a) @C, (b) @TiO_2 and (c) @C-TiO_2 nanocomposite.

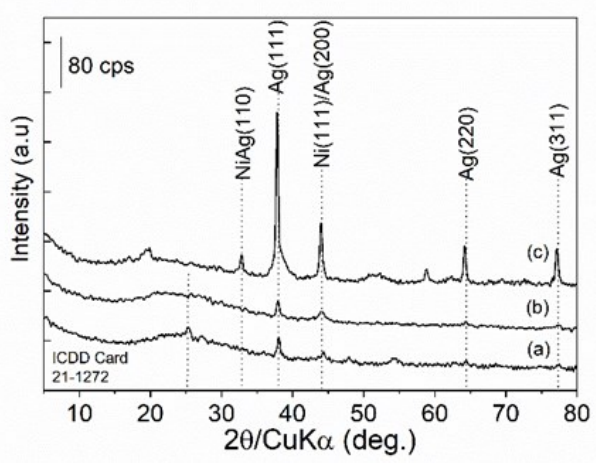

Figure 4. XRD patterns of (a) Ni-Ag(3.0)@C-TiO_2, (b) Ni-Ag(3.0)@TiO_2 and (c) bulk Ni-Ag(3.0).

@TiO_2, @C-TiO_2, Ni-Ag(3.0)@TiO_2 and Ni-Ag(3.0)@C-TiO_2 were 2.96 eV, 2.57 eV, 2.84 eV, and 2.69 eV, respectively. These results indicate that the addition of dopant and co-catalyst significantly shifted the absorption band of @TiO_2 to the visible region as indicated by the E_g.

3.2 Photodegradation of Methylene Blue

Firstly, we carried out the photodegradation of methylene blue (MB) over various catalysts at temperature of 60 °C for 2 h and the results of UV-Vis absorption spectra of the remained MB are shown in Figure 7. By using @TiO_2 catalyst, a the photodegradation of MB was occurred slowly as indicated by a broadened peak of MB species after a reaction time of 2 h. It is found that the synthesized @C-TiO_2 catalyst was not active for MB photodegradation under the same reaction conditions. On the other hand, the amount of MB was significantly reduced in presence of Ni-Ag(3.0)@TiO_2 and Ni-Ag(3.0)/@C-TiO_2 catalysts as indicated by the decreasing of intensity at λ = 664 nm which can be associated as the degradation of phenothiazin functional group and demethylation of N group in MB structure [16].

To obtain insight into the kinetic profiles of each the synthesized catalysts, the photodegradation of MB was monitored using UV-Vis spectrophotometer and the sampling was carried out at interval time of 30 min. The kinetic profiles of MB photodegradation over @TiO_2, @C-TiO_2, Ni-Ag(3.0)@TiO_2, and Ni-Ag(3.0)@C-TiO_2 catalysts are shown in Figures 8. General-

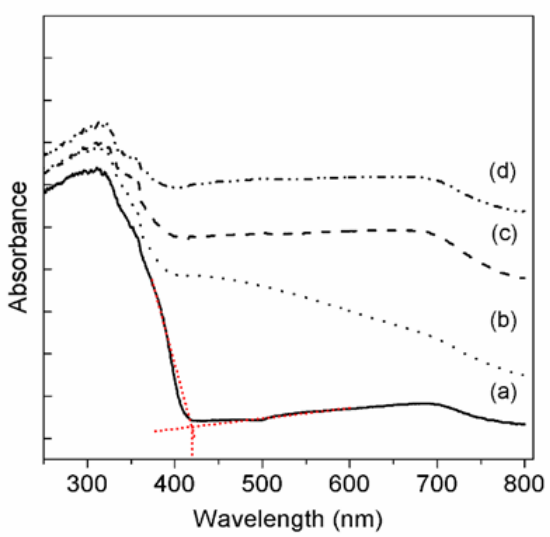

Figure 6. Spectra UV-Vis DRS (a) @TiO_2; (b) @C-TiO_2; (c) Ni-Ag(3.0)@TiO_2, and (d) Ni-Ag(3.0)@C-TiO_2.

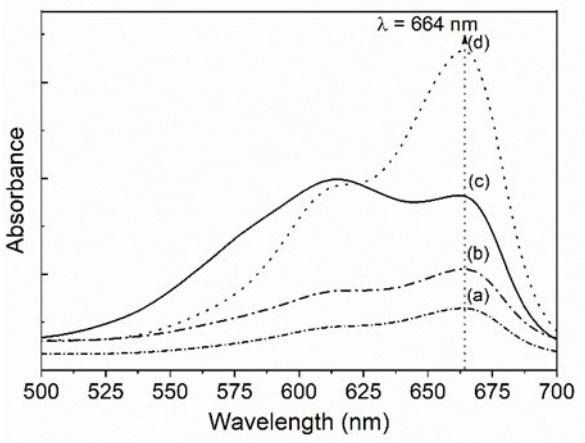

Figure 7. Reaction profiles of MB photodegradation over the synthesized (a) Ni-Ag(3.0)@C-TiO_2, (b) Ni-Ag(3.0)@TiO_2, (c) @TiO_2, and (d) @C-TiO_2 under UV irradiation. *Reaction conditions*: catalyst (0.15 g), MB (100 ppm, 30 mL), reaction time (120 min), at 60 °C.

Tabel 2. Results of MB photodegradation over various photocatalysts under ultraviolet (UV) and visible (Vis) irradiations.

Entry	Catalyst[a]	Irradiation sources	MB (ppm)		Conv.[d] (%)
			Ct_{30}[b]	Ct_{120}[c]	
1	@TiO_2	UV	83.3	40.9	51.0
2	@TiO_2	Vis	53.5	23.4	56.4
3	@C-TiO_2	UV	83.8	74.7	10.9
4	@C-TiO_2	Vis	56.8	48.7	13.5
5	Ni-Ag(3.0)@TiO_2	UV	46.5	21.7	53.4
6	Ni-Ag(3.0)@TiO_2	Vis	27.4	23.4	14.7
7	Ni-Ag@(3.0)C-TiO_2	UV	88.0	28.6	67.5
8	Ni-Ag@(3.0)C-TiO_2	Vis	76.1	34.9	54.1

Reaction conditions: catalyst (0.15 g); MB (100 ppm, 30 mL); reaction time (120 min); reaction temperature (60 °C). [a]Values in the parenthesis are Ni/Ag molar ratio, according to feeding amount. [b]Initial concentration of MB at 30 min. [c]Final concentration of MB after 120 min. [d]Conversion was determined by UV-Vis spectroscopy using a standard curve method.

ly, except @C-TiO_2 catalyst (Figure 8b) exhibited lowest activity for MB photodegradation than the others catalysts. We also intentionally performed the photodegradation reaction of MB under visible irradiation instead of UV using the synthesized catalysts and the results are summarized in Table 2.

The amount of MB after pre-absorption onto the catalyst surface was determined after initial time of 30 min (denoted as Ct_{30}), while the remained MB after a reaction time of 120 min (denoted as Ct_{120}). The conversion of MB was calculated based on the remained MB to Ct_{30} from UV-visible spectroscopic method using standard curve technique. It is found that under UV irradiation, the amount of absorbed MB on the surface of @TiO_2, @C-TiO_2, and Ni-Ag@C-TiO_2 catalysts showed almost similar, which are 83.3 ppm, 83.8 ppm, and 88 ppm. Only Ni-Ag(3.0)@TiO_2 catalyst exhibited very high absorption capacity as indicated by the amount of remained MB after 30 min, *c.a.* 46.5 ppm and 27.4 ppm after irradiation with UV and visible, respectively.

In the case of @TiO_2 catalyst, conversion of MB under UV and visible irradiation was 51.0% and 56.4%, respectively (entries 1 and 2). Consistent with the results of kinetic profiles over @C-TiO_2 catalyst, the conversion of MB was only 10.9% and 13.5% (entries 3 and 4). On the other hand, a relatively high MB conversion was achieved over Ni-Ag(3.0)@TiO_2 after UV irradiation (53.4%, entry 5) while under visible irradiation was only 14.7% (entry 6). Interestingly, Ni-Ag(3.0)@C-TiO_2 demonstrated remarkable high conversion of MB both under UV and visible irradiations. These results suggest that the synergistic action between C dopant and bimetallic Ni-Ag co-catalyst during the MB photodegradation reaction [28-30].

4. Conclusion

We demonstrated the catalytic performance of @TiO_2, @C-TiO_2, Ni-Ag(3.0)@TiO_2, Ni-Ag(3.0)@C-TiO_2 catalysts on the photodegradation of MB under UV and visible irradiations at 60 °C after a reaction time of 120 min. Spectroscopic analysis using UV-Vis DRS confirmed that the addition of C dopant and bimetallic Ni-Ag co-catalyst significantly reduced the band gap energy (E_g) of @TiO_2. The band ener-

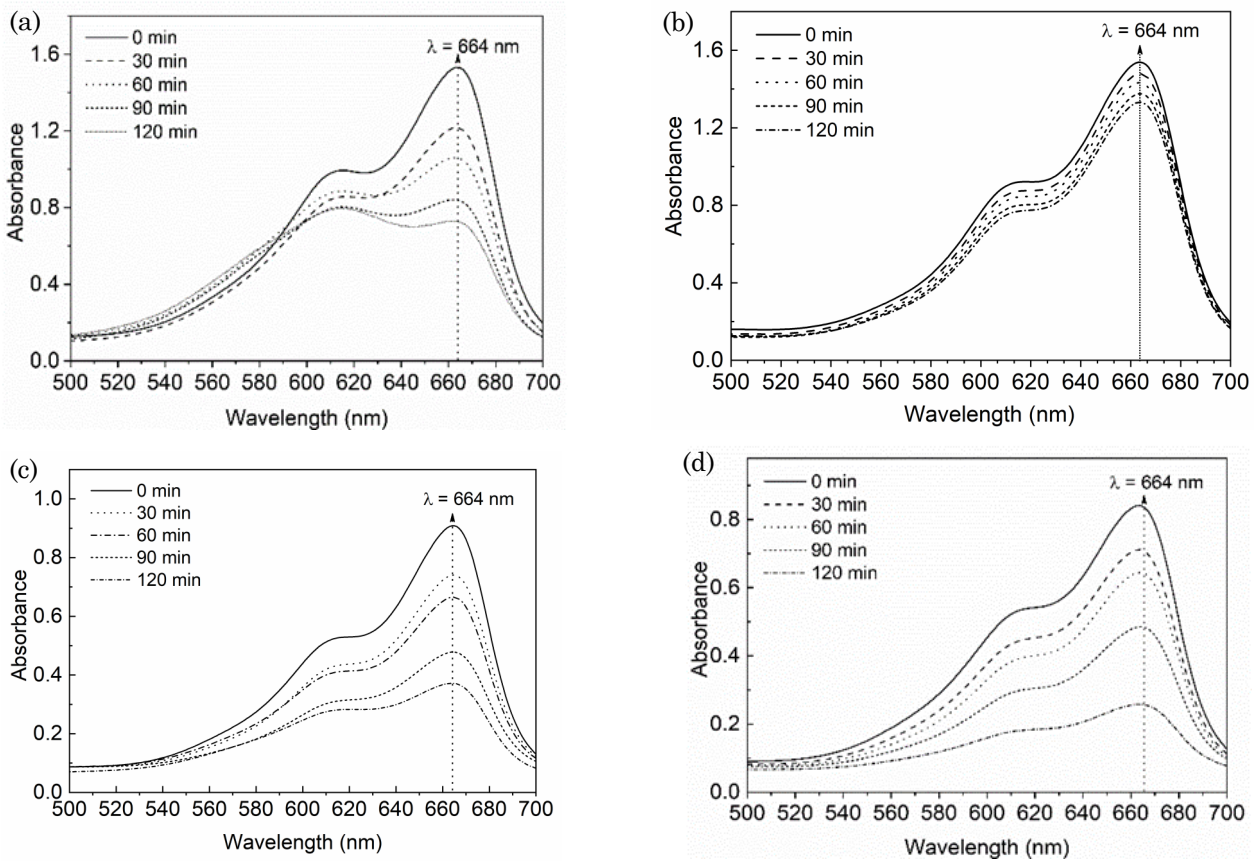

Figure 8. Reaction profiles of MB photodegradation over the synthesized (a) @TiO_2, b) @C-TiO_2, c) Ni-Ag(3.0)@TiO_2, and d) Ni-Ag(3.0)@C-TiO_2 catalysts under UV irradiation. *Reaction conditions*: catalyst (0.15 g), MB (100 ppm, 30 mL), reaction time (120 min), at 60 °C.

gy gap of each synthesized @TiO_2, @C-TiO_2, Ni-Ag(3.0)@TiO_2, Ni-Ag(3.0)@C-TiO_2 catalysts was 2.96 eV, 2.57 eV, 2.84 eV, and 2.69 eV, respectively. Ni-Ag(3.0)@C-TiO_2 catalyst was found to be effective for photodegradation of MB under both UV and visible irradiations with maximum MB conversion of 67.5% and 54.1%, respectively after 120 min.

Acknoledgements

This work was partially supported *Penelitian Berbasis Kompetensi* (PBK) FY 2017-2018 under grant number of DIPA-042.06-1.401516/2018 from Ministry of Research, Technology, and Higher Education, Indonesian Government.

References

[1] Fujishima, A., Rao, T.N., Tryk, D.A. (2000). Titanium Dioxide Photocatalysis. *Journal of Photochemistry and Photobiology C: Photochemistry Reviews*, 1(1), 1–21.

[2] Chen, X., Shen, S., Guo, L., Mao, S.S. (2010). Semiconductor-based Photocatalytic Hydrogen Generation. *Chemical Reviews*, 110(11), 6503–6570.

[3] Kudo, A., Miseki, Y. (2009). Heterogeneous Photocatalyst Materials for Water Splitting. *Chemical Society Review,* 38, 253–278.

[4] Khan, S.U.M., Al-Shahry, M., Ingler., W.B. (2002). Efficient Photochemical Water Splitting by A Chemically Modified n-TiO_2. *Science*, 297(5590), 2243–2245.

[5] Vinodgopal, K., Wynkoop, D.E., Kamat, P.V. (1996). Environmental Photochemistry on Semiconductor Surfaces: Photosensitized Degradation of a Textile Azo Dye, Acid Orange 7, on TiO_2 Particles Using Visible Light. *Environ. Sci. Technol*., 30, 1660-1666.

[6] Zhao, D., Chen, C.C., Wang, Y., Ma, W.H., Zhao, J.C., Rajh, T., Zang, L. (2008). Enhanced Photocatalytic Degradation of Dye Pollutants under Visible Irradiation on Al(III)-Modified TiO_2: Structure, Interaction, and Interfacial Electron Transfer. *Environ. Sci. Technol.*, 42, 308-314.

[7] Fujishima, A., Zhang, X., Tryk, D.A. (2008). TiO_2 photocatalysis and Related Surface Phenomena. *Surface Science Reports*, 63(12), 515–582.

[8] Choi, W., Termin, A., Hoffmann, M.R. (1994). The Role of Metal Ion Dopants in Quantum-Sized TiO_2: Correlation between Photoreactivity and Charge Carrier Recombination Dynamics. *J. Phys. Chem.,* 98, 13669-13679.

[9] Khan, M.A., Woo, S.I., Yang, O.B. (2008). Hydrothermally Stabilized Fe (III) Doped Titania Active Under Visible Light for Water Splitting Reaction. *International Journal of Hydrogen Energy*, 33(20), 5345-5351.

[10] Dholam, R., Patel, N., Adami, M., Miotello, A. (2009). Hydrogen Production by Photocatalytic Water-Splitting Using Cr- or Fe-doped TiO_2 Composite Thin Films Photocatalyst. *International Journal of Hydrogen Energy*, 34, 5337-5346.

[11] Li, Z., Shen, W., He, W., Zu, X. (2008). Effect of Fe-doped TiO_2 Nanoparticle Derived from Modified Hydrothermal Process on the Photocatalytic Degradation Performance on Methylene Blue. *Journal of Hazardous Materials,* 155, 590–594.

[12] Wang, H., Lewis, J.P. (2006). Second-Generation Photocatalytic Materials: Anion-doped TiO_2. *Journal of Physics: Condensed Matter*, 18(2), 421–434.

[13] Chen, D., Jiang, Z., Geng, J., Wang, Q., Yang, D. (2007). Carbon and Nitrogen Co-doped TiO_2 with Enhanced Visible-light Photocatalytic Activity. *Industrial and Engineering Chemistry Research*, 46(9), 2741–2746.

[14] Zhong, J., Chen, F., Zhang, J. (2010). Carbon-Deposited TiO_2 : Synthesis, Characterization, and Visible Photocatalytic Performance. *The Journal of Physical Chemistry C*, 114(2), 933–939.

[15] Teng, F., Zhang, G., Wang, Y., Gao, C., Chen, L., Zhang, P., Zhang, Z., Xie,E. (2014). The Role of Carbon in The Photocatalytic Reaction of Carbon/TiO_2 Photocatalysts. *Applied Surface Science*, 320, 703–709.

[16] Zuo, R., Du, G., Zhang, W., Liu, L., Liu, Y., Mei, L., Li, Z. (2014). Photocatalytic Degradation of Methylene Blue Using TiO_2 Impregnation Diatomite. *Advances in Materials Science & Engineering,* 1, 1-7.

[17] Jing, D., Zhang, Y., Guo, L. (2005). Study On The Synthesis of Ni Doped Mesoporous TiO_2 and Its Photocatalytic Activity for Hydrogen Evolution in Aqueous Methanol Solution. *Chemical Physics Letters*, 415, 74–78.

[18] Yang, J., Wang, D., Han, H., Li, C. (2013). Roles of Cocatalysts in Photocatalysis and Photo electrocatalysis. *Accounts of Chemical Research*, 46(8), 1900-1909.

[19] Zhang, D. (2011). Chemical Synthesis of Ni/TiO_2 Nanophotocatalyst for UV/Visible Light Assisted Degradation of Organic Dye in Aqueous Solution. *Journal of Sol-Gel Science and Technology*, 58(1), 312–318.

[20] Sung-Suh, H.M., Choi, J.R., Hah, H.J., Koo, S.M., Bae, Y.Cer. (2004). Comparison of Ag Deposition Effects on The Photocatalytic Ac-

tivity of Nanoparticulate TiO_2 Under Visible and UV Light Irradiation. *Journal of Photochemistry and Photobiology A: Chemistry*, 163(1-2), 37–44.

[21] Aritofa, R. (2014). Synthesis and Characterization of Ni-Ag(0.75) Nanoalloy Catalyst Supported on Al_2O_3 : Variation of Ethylene Glycol. *Skripsi Program Strata-1, Universitas Lambung Mangkurat, Banjarbaru*.

[22] Rodiansono, R., Astuti, M.D., Santoso, U.T., Irwan, A., Mujiyanti, D.R., Aritofa, R. Karlini, K., Abdurahman, A., Maulana, A. (2018). Controlled-Selectivity of Bimetallic Ni-Ag Alloy Catalysts in Hydrogenation of Furfural to Furfuryl Alcohol and Tetrahydrofurfuryl Alcohol. *Sains dan Terapan Kimia.* 12(2), 41- 53.

[23] Jiao, W., Xie, Y., Chen, R., Zhen, C., Liu, G., Ma, X., Cheng, H.M. (2013). Synthesis of Mesoporous Single Crystal Rutile TiO_2 with Improved Photocatalytic and Photoelectrochemical Activities. *Chem. Commun.,* 49, 11770-11772.

[24] Ren, W., Ai, Z., Jia, F., Zhang, L., Fan, X., Zhou, Z. (2007). Low Temperature Preparation and Visible Light Photocatalytic Activity of Mesoporous Carbon-doped Crystalline TiO_2. *Applied Catalysis B: Environmental*, 69(3-4), 138–144.

[25] Powder diffraction files. (1997). *JCPDS-International center for diffraction data (ICDD).*

[26] Zhang, Y.W., Si, R., Liao, C.S., Yan, C.H. (2003). Facile Alcohothermal Synthesis, Size-dependent Ultraviolet Absorption, and Enhanced CO Conversion Activity of Ceria Nanocrystals. *J. Phys. Chem. B.,* 107, 10159–10167.

[27] Ng, J., Xu, S., Zhang, X., Yang, H.Y., Sun, D.D. (2010). Hybridized Nanowires and Cubes: A Novel Architecture of A Heterojunctioned $TiO_2/SrTiO_3$ Thin Film for Efficient Water Splitting. *Adv. Funct. Mater.,* 20, 4287–4294.

[28] Ma, Y., Wang, X., Jia, Y., Chen, X., Han, H. Li, C. (2014). Titanium Dioxide-Based Nanomaterials for Photocatalytic Fuel Generations. *Chem. Rev.*, 114, 9987−10043.

[29] Pal, U., Ghosh, S., Chatterjee, D. (2012). Effect of Sacrificial Electron Donors on Hydrogen Generation Over Visible Light-Irradiated Nonmetal-doped TiO_2 Photocatalysts. *Transition Metal Chemistry*, 37(1), 93–96.

[30] Silva, C.G., Jua´rez, R., Marino, T., Molinari, R., Garcı´a, H. (2011). Influence of Excitation Wavelength (UV or Visible Light) on the Photocatalytic Activity of Titania Containing Gold Nanoparticles for the Generation of Hydrogen or Oxygen from Water. *J. Am. Chem. Soc.*, 133, 595–602.